# Journal of Applied Polymer SCIENCE

# Phosphorous Antioxidants Against Polypropylene Thermal Degradation During Rotational Molding-Kinetic Modeling

Salah Sarrabi, Marie-France Lacrampe, Patricia Krawczak

Mines Douai, Department of Polymers and Composites Technology & Mechanical Engineering, F-59508 Douai, France
Correspondence to: S. Sarrabi (E-mail: sssarabi@gmx.com)

**ABSTRACT:** Phosphorous antioxidants efficiency against molten polypropylene (PP) thermal oxidation was assessed during isothermal ageing and processing by rotational molding. During isothermal ageing, experimental data were compared to the ones calculated on the basis of a kinetic model. Phosphonite is more effective than phosphite. Both phosphite and phosphonite decompose hydroperoxide and prevent initiation of oxidation reactions. However, phosphonite hydrolysis product acts as a radical chain terminator and blocks propagation reactions. Kinetic constants of stabilization reactions were evaluated and discussed. Further, this kinetic modeling was coupled to a thermal software, able to predict polymer temperature evolution during rotational molding and the degradation critical temperature (DCT) of different stabilized PP. A DCT of 235°C was obtained for PP stabilized with phosphonite and hindered phenol against 215°C for PP stabilized with phosphite and the same phenol. This difference of 20°C, corresponding to 5 min more heating is significant to optimize rotational molding. © 2014 Wiley Periodicals, Inc. J. Appl. Polym. Sci. **2015**, *132*, 41285.

## INTRODUCTION AND BACKGROUND

### Standard Scheme

Polypropylene (PP) is a semicrystalline polymer often used in industry for its better mechanical performance in comparison with polyethylene (PE). Compared with PE, one major drawback of PP is its hig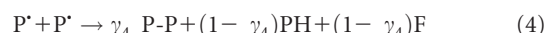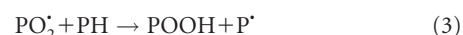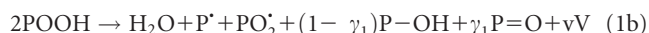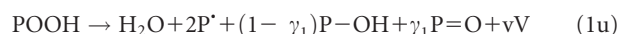h sensitivity to thermal oxidation.[1] Since 1940s, there is a general agreement on the radical character of hydrocarbon substances oxidation reactions,[2,3] Bolland[2,4] was pioneer in the field. This scheme is also called standard scheme.[5–7] Thermal oxidation reaction begins with alkyl radical formation ($P^\bullet$), which then reacts with oxygen $O_2$ to form peroxyl radicals $PO_2^\bullet$ [reaction (2)]. The alkyl radical $P^\bullet$ in reaction (3) results from abstraction of a labile Hydrogen from polymer, noted PH. The resulting hydroperoxide POOH [reaction (3)] is then decomposed by unimolecular [reaction (1) with $\delta = 1$, $\alpha = 2$, and $\beta = 0$] or bimolecular reaction [reaction (1) with $\delta = 2$, $\alpha = 1$, and $\beta = 1$]. As long as there is oxygen $O_2$,[8] there is formation of a closed-loop:[5] oxidation reactions produce their own initiator POOH. Termination reactions (4–6) involve the different radicals.

### Standard Scheme Extended to PP in Molten State

Standard scheme predicts polymers thermal oxidation in long-term use condition,[9–13] that is, when the polymer is in solid state.[14–17] More recently, standard scheme was extended to higher temperatures,[18] where polymer is in molten state. This scheme is written, in the case of PP in molten state, as follows:[18]

$$POOH \rightarrow H_2O + 2P^\bullet + (1-\gamma_1)P-OH + \gamma_1 P=O + vV \quad (1u)$$

$$2POOH \rightarrow H_2O + P^\bullet + PO_2^\bullet + (1-\gamma_1)P-OH + \gamma_1 P=O + vV \quad (1b)$$

$$P^\bullet + O_2 \rightarrow PO_2^\bullet \quad (2)$$

$$PO_2^\bullet + PH \rightarrow POOH + P^\bullet \quad (3)$$

$$P^\bullet + P^\bullet \rightarrow \gamma_4 \ P\text{-}P + (1-\gamma_4)PH + (1-\gamma_4)F \quad (4)$$

$$P^\bullet + PO_2^\bullet \rightarrow \gamma_5 POOP + (1-\gamma_5)POOH + (1-\gamma_5)F \quad (5)$$

$$PO_2^\bullet + PO_2^\bullet \rightarrow [PO^{\bullet\bullet}OP]_{cage} + O_2 \quad (6.0)$$

$$[PO^{\bullet\bullet}OP]_{cage} \rightarrow POOP \quad (6.1)$$

$$[PO^{\bullet\bullet}OP]_{cage} \rightarrow \ 2P^\bullet + 2\gamma_1 P=O + 2(1-\gamma_1)P\text{-OH} + 2 \ vV \quad (6.3)$$
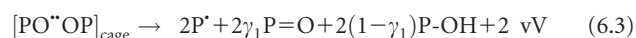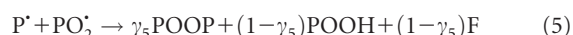
- $H_2O$ is water,
- $V$ is an average volatile compound, formed by $\beta$ scission with yield $v$. Acetone is considered, in first approximation, as major Volatile Organic Compound,[19]

- $\gamma_1$ is yield of ketone, noted P = O,
- F represents a double bond and $\gamma_4$ is yield of alkyl–alkyl (P–P) bridges,
- $\gamma_5$ is yield of peroxide bridges, noted POOP,
- $[PO\ddot{}OP]_{cage}$ is a tetraoxyde,[20] unstable compound, which led to ketone and alcohol by Russel mechanism.[21]

The writing of initiation reactions may seem surprising (as the stoichiometry is not respected), but there are numerous intermediate reactions.[22] Moreover, termination reaction (6) described in solid state cannot be efficient in molten state, as described elsewhere.[18] Actually, it is more reasonable to consider that a non negligible part of radical pairs could escape from cage [reaction (6.3)]. Finally, his new model remains valid between polymer melting temperature and 250°C, beyond which thermolysis of PP is significant.[23]

### Standard Scheme for PP in Molten State and Extended to Antioxidants

Polymer grades used in industry are never unstabilized. They always contain antioxidants that inhibit and retard thermal oxidation reactions, particularly during processing.[24] "Radical chain terminators" and "preventive antioxidants" are two major antioxidants families used in PP[25–27] and other polymers.[28–30]

Radical chain terminators are able to increase termination rate.[6,31–33] They are the most common Hydrogen donors. Radical chain terminators are hindered phenols or secondary aromatic amines. They are particularly effective in service condition.[33] They contain one (or more) Hydrogen (s) more labile (s) than those from substrate (PH). That is why radical chain terminators are noted AH. For example, in case of hindered phenols, dissociation energy of bond A—H is 335–355 kJ mol$^{-1}$,[34–36] against 380–395 kJ mol$^{-1}$ for P—H bond from polyolefins. This family of antioxidants releases Hydrogen to a peroxyl radical $PO_2^{\cdot}$ easier. Their mechanism of action is written as follows:[31–33]

$$PO_2^{\cdot}+AH \rightarrow POOH + A^{\cdot} \qquad (7.0)$$
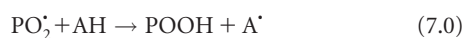
Note that radical $A^{\cdot}$ formed is unable to initiate new reactions, even if reality is more complex.[37,38] Numbers of authors have focused on phenolic antioxidants. However, there is few kinetic data. According to Gol'dberg et al.,[39] activation energy ($E_a$) of reaction (7.0) is 20.5 kJ mol$^{-1}$.

Preventive antioxidants are able to decrease initiation rate.[33] They are used to prevent oxidation initiation. The most common preventive antioxidants are hydroperoxide decomposers acting by nonradical way. In polyolefins, they are usually organic phosphites (noted Dec). They are effective during polymer processing (typically when $T > 200°C$[33,40–45]). As a first approximation, their mechanism of action is written as follows,[33,34] even if the reality is more complex:[46–50]

$$POOH+Dec \rightarrow IP^* \qquad (8.0)$$

IP* = Inactive products

The family of organic phosphites is a set of non hydrolyzable organic compounds such as Tris (2,4-di-tert-butylphenyl)

phosphite or phosphine and hydrolyzable organic compounds such as phosphonite. Literature often compares effectiveness of organic phosphites in PE. For example, efficiency of melt stabilising phosphonite in PE is larger than that from phosphate.[43] Phosphonite and phosphine hinder efficiently formation of long chain branches above the critical residual concentration of 200 ppm.[43] During LLDPE extrusion at 265°C, Al Malaika and Peng[51] show that phosphonite is less effective than phosphite. To our best knowledge, Costanzi et al.[52] have been the only authors who compared the efficiency of organic phosphites against PP thermal oxidation. They reported that phosphite content in PP is consumed faster than phosphonite during a dynamic heating at 10°C min$^{-1}$. Actually, phosphonite can hydrolysis at high temperature as follows:[48]

$$Dec \xrightarrow{H_2O} BH+IP^* \qquad (9)$$

IP* = Inactive products

Product of reaction (9) is BH, a radical chain terminator able to react with peroxyl radical following reaction (7.1):

$$PO_2^{\cdot}+BH \rightarrow POOH+IP^* \qquad (7.1)$$

IP* = Inactive products

Rate constants of peroxyl radical reaction with BH (from organic phosphite hydrolysis) are 10–100 times smaller than values of hindered phenols at temperature inferior to 100°C.[53] In summary, the decomposition of hydroperoxide by a phosphorous antioxidant is a fast reaction.[49] Its rate is affected by antioxidant chemical structure. It decreases with electron-acceptor ability and bulk of group bonds to phosphorus atom in the following order: phosphonites > phosphites.[49,54] However, its rate depends also on the structure and morphology of polymer and thermal conditions also.[55] The efficiency of different organic phosphites in PP was rarely compared. Furthermore, the efficiency of preventive antioxidants during PP processing by rotational molding, where thermal condition is the most aggressive[56] as described below, has not been described yet.

### Rotational Molding

Rotational molding is a polymer processing technique used to manufacture hollow parts.[56] Its principle is relatively easy.[57] Polymer, in a powder form, is introduced into a mold. Then, mold in rotation goes inside an oven to be heated. After that, the mold, which contains molten polymer enters a cooling room. Finally, when internal air temperature (in mold center) is sufficiently low, part is removed. To monitor these steps, a solution consists in placing a thermosensor in internal air and measuring evolution of temperature with time.[58,59] The associated curve is called Temperature-time diagram or $Tt$ diagram. Indirectly, it reflects polymer state changes during processing. To optimize rotational molding, some authors developed models[60–66] to simulate $Tt$ diagram. Today, the latest model correctly predicts $Tt$ diagram with an error <1% between theory and experiment.[66] Thermal and chemical models were also coupled to describe PP thermal oxidation

**Table I.** Main Characteristics of the Neat PP Studied (from Datasheets)

| Physical | Standard | Value |
|---|---|---|
| Density | ISO 1183 | 0.9 (g cm$^{-3}$) |
| Melt flow rate (MFR) (230°C/2.16 kg) | ISO 1133 | 15 (g 10 min$^{-1}$) |
| Mechanical | | |
| Tensile stress at yield (50 mm/min) | ISO 527-1, −2 | 23 (MPa) |
| Flexural modulus (Secant) | ISO 178 | 1100 (MPa) |

during processing by rotational molding.[67] Results show that molten PP stabilized with phosphite (Irgafos 168) and hindered phenol (Irganox 1010) is thermally degraded above 20 min of heating at 300°C (oven temperature). The degradation critical temperature (DCT) of this stabilized PP was estimated at 215°C.[67]

To increase PP processing domain, a solution is to add a more effective antioxidant. Phosphonite seems to be more appropriate, in these conditions, than common phosphate.[52] In this study, the efficiency of preventive antioxidants against PP thermal degradation was investigated in rotational molding thermal condition using numerical method.

## THEORETICAL BACKGROUND

### Thermal Modeling
A previous article[66] described a thermal model (1D) that simulates evolution of polymer temperature during processing. This model was based on finite differences method using a centered implicit scheme for space and a decentred implicit scheme for time. It was then integrated using an implicit Euler algorithm of order 1. Equations and interfaces were treated with the same system. Calculated results from this thermal model were computed using Matlab with the assumptions described before.[66]

### Chemical Modeling
The kinetic model extended to molten polymer stabilized by phosphonite and phenol antioxidants, derived from reaction scheme described in the Introduction section is presented in Appendix 1. Ode23s Matlab solver was used to solve the system of eqs. (A1–A16), see Appendix 1, with the following boundary conditions:

■ In thickness, whatever $x$, when $t=0$:
$[P^\bullet]=[PO_2^\bullet]=[PO^{\bullet\bullet}OP]=[H_2O]=[P\text{-}OH]=[P=O]=[V]=[PP]=[F]=[POOP]=[BH]=0$ mol L$^{-1}$; $[POOH]=[POOH]_0$; $[PH]=[PH]_0=20.3$ mol l$^{-1}$,[18]; $[O_2]=[O_2]_0=P_{O2}\times S$ (Henry law), $P_{O2}$ is partial pressure of $O_2$ in atmosphere and $S$ solubility coefficient of $O_2$ in polymer; $[Dec]=[Dec]_0$; $[AH]=[AH]_0$.
■ On surface in contact with oxygen from air (at $x=0$), when $t>0$, $[O_2]=[O_2]_S=P_{O2}\times S$ (oxygen dissolution is instantaneous at inner polymer surface),

$$D_{Dec}\frac{\partial^2[Dec]}{\partial x^2}=-\beta_{Dec}[Dec]$$

$$D_{AH}\frac{\partial^2[AH]}{\partial x^2}=-\beta_{AH}[AH]$$

$$D_{BH}\frac{\partial^2[BH]}{\partial x^2}=-\beta_{BH}[BH]$$

Antioxidants leave inner polymer surface with a rate proportional to their concentration. $\beta_{Dec}$, $\beta_{AH}$, and $\beta_{BH}$ are the coefficient of crossing by both types of antioxidants ($=10^{-5}$ s$^{-1}$ for organic phosphites and hindered phenol antioxidants[18]).
On opposite surface, in contact with mold (at $x=e_p$), when $t>0$: flows of oxygen and antioxidants are null.

The system constituted of eqs. (A1)–(A13), Appendix 1, gives access to spatial distribution in thickness of concentration of primary products and their evolution with time. Equations (A14–A16) provide access to distribution of [P—O], [P—OH] and mass loss. Finally, assuming that the sample thickness $e_p$ does not vary during exposure, evolution of global secondary product quantities may be determined by summing contribution of each elementary layer:

$$[y]_{glob}(t)=\frac{1}{e_p}\int_0^{e_p}[y](x,t)dx$$

where $[y]=[P=O]$, $[P\text{-}OH]$, or mass loss and $e_p$ is sample thickness.

In this article, hydroxyl concentration [P—OH] was not studied due to its high sensibility to humidity and the badly defined band observed in infrared analysis (IR).[18]

In a first part, chemical modelling was used alone to identify the kinetic constants $k_x(T)$ of all elementary reactions during isothermal condition ageing. Actually, in a given polymer physical state, $k_x(T)$ obeys to Arrhenius law:

$$k_x(T)=k_0\exp\left(-\frac{E_a}{RT}\right)$$

where $k_0$ and $E_a$ are, respectively, pre-exponential factor and activation energy.

Thanks to inverse method, which compares experimental and numerical results, kinetic constants were determined for each ageing temperature studied (in isothermal condition). Then, the kinetic parameters ($k_0$, $E_a$) of each elementary reaction were deduced by plotting ln $k_x=f(1/T)$ and used for the ageing modeling during processing.

In a second part, chemical model was coupled with the previously developed thermal model (see Thermal Modeling section) to estimate parts thermal oxidation in real thermal condition during rotational molding. In this section, only theoretical results were presented, no real parts were manufactured. This aims at investigating the stabilization mechanisms of phosphorous antioxidants against molten PP thermal oxidation during rotational molding.

**Table II.** Some Thermal Characteristics of the Neat PP Studied

| Property | Technique (condition) | Value |
|---|---|---|
| $T_f$ | DSC (10°C min$^{-1}$) | 167 (°C) |
| $T_C$ | DSC (N$_2$, 20°C min$^{-1}$) | 127 (°C) |
| $X_c$ | IR | 40 (%) |

Melting temperature ($T_f$), crystallization temperature ($T_c$), and degree of crystallinity ($X_c$).

## EXPERIMENTAL

### Materials

The PP studied was an isotactic (PP 1752, Icopolymers). It is provided under powder form. Table I shows the properties. The radical chain terminator used is a hindered phenol (Irganox 1010, Basf). The preventive antioxidant added to PP is either a phosphonite (PEPQ, Clariant) or a phosphite (Everfos 168, Everspring).

To have equal reactivity, the following assumption was made: antioxidant is dissolved only in amorphous phase.[68] Antioxidant concentration, noted [Dec], was then deducted from following total mass fraction:

$$[\text{Dec}] = f_{\text{Dec}} \frac{1}{1-X_c} \frac{m_{\text{Dec}}/M_{\text{Dec}}}{m_{\text{pp}}/d_{\text{pp}}} \quad (68)$$

with $f_{\text{Dec}}$ phosphorus functionality (1 for phosphite and 2 for phosphonite), $m_{\text{Dec}}$ and $m_{\text{PP}}$ are mass of additive and polymer respectively, $M_{\text{Dec}}$ is molecular weight of antioxidant (647 g mol$^{-1}$ for phosphite and 1035 g mol$^{-1}$ for phosphonite), $d_{\text{PP}}$ is density of PP (900 g L$^{-1}$) (see Table I) and $X_C$ is the degree of crystallinity of PP. In terms of reaction, a concentration of phosphite of 0.3% corresponds to a phosphonite concentration of 0.25% for an initial concentration, noted $[\text{Dec}]_0$ of $10^{-2}$ mol L$^{-1}$. After dosing, polymers were mixed during 10 min by hand and then extruded in a micro-extruder (Haake Minilab II, Thermoscientific) at 180°C. The screw rotation speed was set at 70 rpm. The extrudates obtained were pressed at 200°C, 16 MPa during 5 s to obtain films with an average thickness of 50 ± 5 µm.

### Characterization Methods

**Differential Scanning Calorimetry (DSC).** Calorimetry analysis was carried out thanks to a DSC device (DSC7, Perkin Elmer), calibrated with indium. The following experimental procedure was used:

- Heating from ambient to 250°C with a rate of 10°C min$^{-1}$,
- 2 min isothermal plateau at 250°C,
- Cooling under N$_2$ (50 mL min$^{-1}$) with a rate of 20°C min$^{-1}$.

**Infrared Analysis.** A Fourier-transform infrared spectroscopy (FTIR) analyser (Nicolet 380 FT-IR, Thermo Scientific, with OMNIC software for data collection and analysis) was used in transmission mode. The spectral range studied extends from 4000 to 400 cm$^{-1}$ with a spectral resolution of 4 cm$^{-1}$.

At first, IR equipment was used to characterize initial polymer crystallinity ratio using Samuels's law:[69]

$$X_c(\%) = 100 \times \left[ 109 \left( \frac{\text{DO}_{997} - \text{DO}_{907}}{\text{DO}_{972} - \text{DO}_{907}} \right) - 31.4 \right]$$

$\text{DO}_x$ is the measured absorbance on peak at a wave number $x$. For this measure, films were used (see Materials section).

Second, IR equipment was used to characterize thermal oxidation of stabilized specimens. The stabilized polymer films obtained in Materials section were aged in ventilated oven in isothermal condition during 10 or 30 min depending on ageing temperature (i.e., 30 min for $T < 220$°C and 10 min for $T > 220$°C). Samples were first placed on a KBr pellet (transparent in infrared spectroscopy) to prevent flowing inside ageing equipment then removed from furnace at different times to be analysed by IR. No precautions were taken to avoid thermal oxidation during transfer between oven and IR equipment. Here, the aim was to measure absorbance evolution of carbonyl groups (P=O) that appear during ageing at 1713–1722 cm$^{-1}$.[70–74] The following Beer-Lambert law allows connecting absorbance DO with concentration [P=O]:

$$[\text{P=O}] = \frac{\text{DO}}{L\varepsilon}$$

where DO is the measured absorbance, $L$ sample thickness, and $\varepsilon$ molar extinction coefficient ($\varepsilon_{\text{CO}} = 200$ L mol$^{-1}$ cm$^{-1}$; Ref. 74).

### Thermogravimetric Analysis (TGA)

At same time, other films were placed in TGA oven (TGA7, Perkin Elmer) for ageing in same conditions that in IR analysis. Mass changes were monitored for temperatures between 200 and 250°C with the following thermal protocol:

- Fast rise until ageing temperature (heating rate of 40°C min$^{-1}$). No precautions were taken to avoid thermal oxidation during this step,
- Isothermal plateau during 10 or 30 min at ageing temperature,
- Cooling until ambient temperature at a rate of 40°C min$^{-1}$.

## RESULTS AND DISCUSSION

### Initial Characterization

The measured thermal properties of the neat PP were shown on Table II. Those parameters are essential for simulation.

### IR Analysis

IR spectra of neat PP and stabilized PP (with phosphonite or phosphite) were presented in Figures 1 and 2. Three peaks appear only on the stabilized PP spectra and can this be attributed to the antioxidants.[75,76] They are located 1195, 1080, and 770 cm$^{-1}$. There is also a fourth band near to 850 cm$^{-1}$ corresponding to P—O—C bond.[75]

Moreover, over 50 measurements at different locations on same film or other films were made to check the compound homogeneity. However, even if small bands are observed in IR spectra, they do not allow a quantitative measure. Thus, consumption of
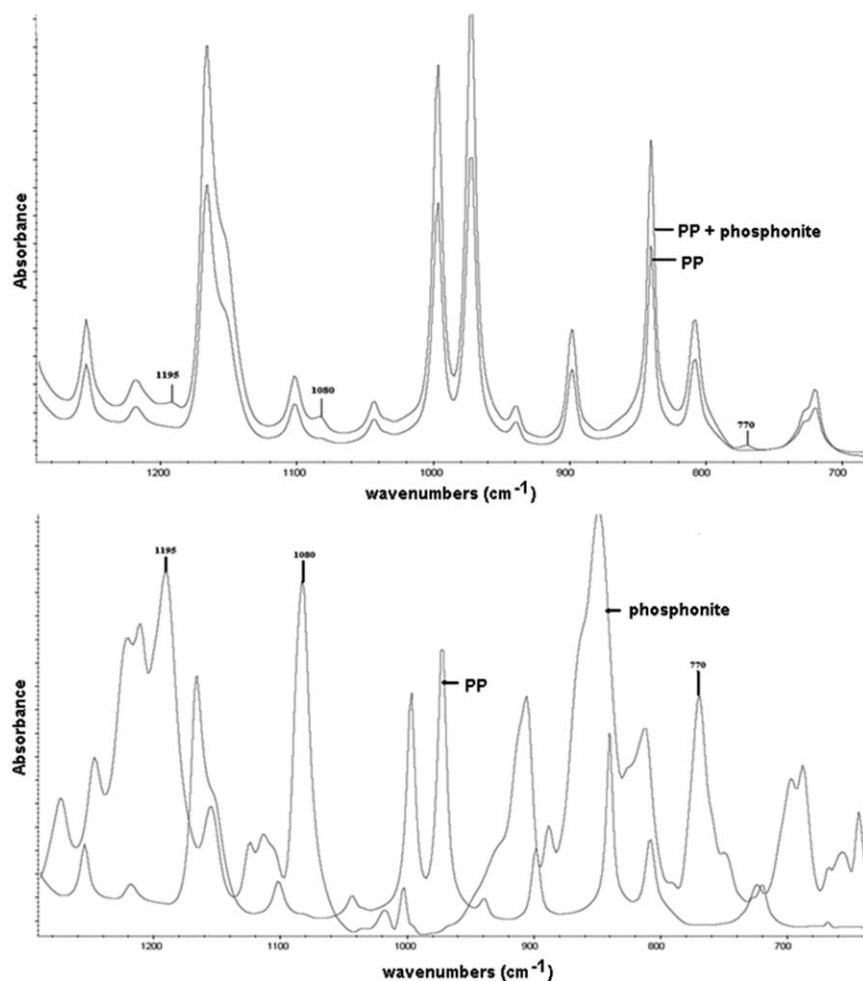
**Figure 1.** Characteristic IR peaks of phosphonite in PP.

antioxidants during ageing will not be simulated in next sections.

### Thermal Ageing

Figure 3 shows IR spectra obtained during ageing of unstabilized PP at 250°C for different times. PP has undergone chemical changes which result in emergence of one peak at 1716 cm$^{-1}$ indicating the presence of P=O from carbonyl groups of ketones.[77] From Beer-Lambert law, evolution of [P=O] was plotted for the three grades aged in the same conditions. The evolution of the mass loss of the same materials was also plotted (Figure 4). Oxidation Induction Time (OIT) obtained by IR and TGA are similar. For example, an OIT of 60 s in TGA against 50 s in IR was measured for neat PP. Experimental protocol was similar for both analysis (IR and TGA). Table III reports OIT measured for temperatures ranging from 200 to 250°C. OIT of PP grade stabilized with phosphonite are at least two times higher than OIT of PP grade stabilized with phosphite (for $T < 250°C$). This difference increases when temperature decreases. OIT of PP grade stabilized with phosphonite are at least three times higher than OIT from neat PP and the difference increases when temperature decreases. Also, note that above the critical temperature

of 215°C (here, 220°C), phosphite is practically consumed while phosphonite still protects PP against thermal degradation. Moreover, note in Figure 4 that the maximum slope of mass changes curves is lower for PP stabilized with phosphonite, showing that PP oxidizes less rapidly in presence of phosphonite, according to literature.[52]

In summary, phosphonite seems to better protect PP against thermal degradation at temperatures encountered during processing by rotational molding, even it is known that isothermal aging of thin films at high temperature in air-ventiled ovens or TGA cavity is not completely representative of aging in real processing conditions The next section is dedicated to the identification of kinetic constants of the stabilization reactions with phosphite or phosphonite antioxidant in isothermal condition and in real thermal condition during rotational molding.

### Kinetic Modeling

**In Isothermal Condition.** Figure 5 compares calculated and experimental evolution of [P=O] and mass losses during isothermal ageing of PP grade stabilized with phosphite for temperatures ranging from 200 and 250°C. The model correctly predicts the evolution of ageing indicators, and particularly the
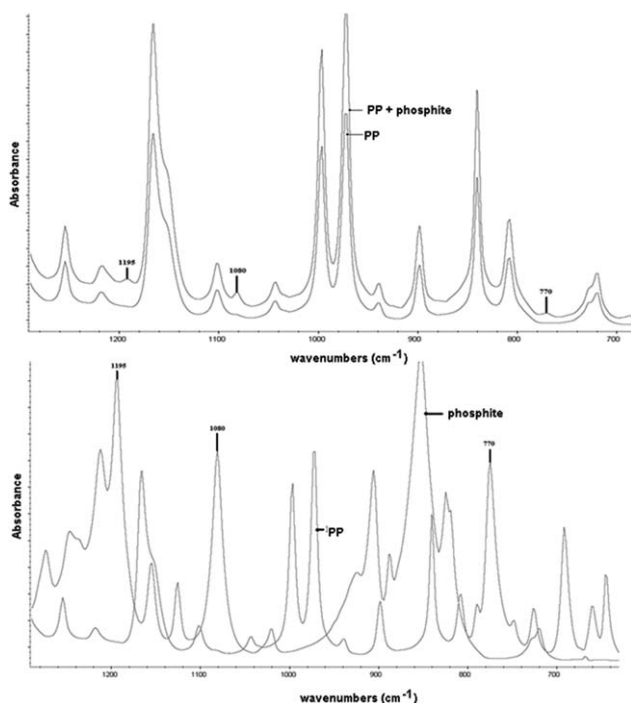
**Figure 2.** Characteristic IR peaks of phosphite 168 in PP.

induction period and the acceleration at end of the induction period for all temperatures. The following reaction was added to the thermal oxidation reaction scheme of neat PP in molten state:[18]

$$POOH + Dec \rightarrow Inactive\ Products \qquad (8.0)$$

Kinetic constants of stabilization reaction (8.0) and of elementary reactions of PP thermal oxidation in molten state are reported in Table IV.

**Results Refer to Following Comments**

All kinetic curves show an induction period. Direct action of oxygen with polymer is negligible at these temperatures. Decomposition of hydroperoxide initiates thermal oxidation, even if initial hydroperoxide concentration $[POOH]_0$ is minimal. Here, $[POOH]_0 = 10^{-3}$ mol L$^{-1}$ (measured by titration[78]). Propagation rate constants $k_2$ and $k_3$ were determined by structure-properties relationships.[33] The corresponding kinetic constants are very fast: $k_2 = 10^8 - 10^9$ L mol$^{-1}$ s$^{-1}$ and the activation energy is null.[31] For calculations, a value of $10^8$ L mol$^{-1}$ s$^{-1}$ was chosen. Arrhenius parameters of constant $k_3$ were determined from Korcek relations[79]: $E_3 = 3.10^8 \exp\left(-\dfrac{65500}{RT}\right)$. Here, $k_3/k_2 = 1.8 \times 10^{-7} = 10^{-8}$. Regarding volatile compounds, acetone was considered as main volatile from PP thermal oxidation.[19] Therefore, $M_V = 58$ g mol$^{-1}$, $n_{CO} = 1$, $n_{OH} = 0$, and $n_{PH} = 0$.

All other model parameters were determined by inverse method. All values seem relevant. Rate constants of termination respect hierarchy theory: $k_4 > k_5 >> k_{60}$.[16] Magnitude of activation energies and pre-exponential factors correspond to those

previously reported in literature.[11,12,80–83] For unimolecular (1u) and bimolecular (1b) decomposition reactions, the obtained values confirm following inequalities:

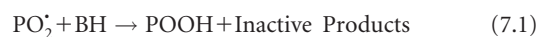$$E_{1u} > E_{1b} \text{ with } E_{1u} = 120 - 150 \text{ kJ mol}^{-1}$$

$$E_{1b} = 80 - 110 \text{ kJ mol}^{-1}. k_{1u0} > k_{1b0} \text{ with } k_{1u0} = 10^{11} - 10^{14} \text{ s}^{-1} \text{ and}$$

$$k_{1b0} = 10^8 - 10^{11} \text{ L mol}^{-1}\text{s}^{-1}$$

Regarding kinetic constants of bimolecular reactions combinations of peroxyl radicals, the obtained values confirm following hierarchy: $E_{63} > E_{61} > E_5 \geq E_4$ with $E_{63} = 20–50$ kJ mol$^{-1}$, $E_{61} = 0–20$ kJ mol$^{-1}$ and $E_5 = E_4 = 0$ kJ mol$^{-1}$ and following order: $k_{40} > k_{50}$. $k_{610} = 10^8 - 10^{11}$ L mol$^{-1}$ s$^{-1}$, $k_{630} = 10^9 - 10^{13}$ s$^{-1}$.

Concerning stabilization reaction (8.0), activation energy (80 kJ mol$^{-1}$; Ref. 67) is reasonably inferior to activation energy of reaction (1b). Here, $E_{1b} = 108$ kJ mol$^{-1}$. The order of magnitude of pre-exponential factors ($10^7 - 10^{10}$ L mol$^{-1}$ s$^{-1}$) corresponds well to that usually reported in the literature for bimolecular reactions.[80–83] For comparison, Richaud and coworkers[76] obtained, in solid state and for a similar $[Dec]_0$, an activation energy of 100 kJ mol$^{-1}$ and a pre-exponential factor of $1.2 \times 10^{13}$ L mol$^{-1}$ s$^{-1}$. At 200°C, the constant obtained here is six times inferior to Richaud extrapolation from solid state. Moreover, the more the temperature increases, the more this ratio increase (10 times inferior at 250°C).

Figure 6 compares calculated and experimental evolution of [P=O] and mass losses during isothermal ageing of PP stabilized with phosphonite for temperatures ranging from 200 to 250°C. The following reactions were added to the mechanistic scheme of neat PP thermal oxidation in molten state:[18]

$$POOH + Dec \rightarrow Inactive\ Products \qquad (8.1)$$

$$Dec \xrightarrow{H_2O} BH + Inactive\ Products \qquad (9)$$

$$PO_2^{\bullet} + BH \rightarrow POOH + Inactive\ Products \qquad (7.1)$$

Dec means phosphonite in this section. It decomposes hydroperoxide in reaction (8.1) and product of Dec hydrolysis is BH. BH decomposes peroxyl radical in reaction (7.1).

Kinetic constants of these different stabilization reactions were shown on Table V. Values of kinetic constants (8.1) obtained for each temperature are smaller than those obtained for hydroperoxide decomposition by phosphite (8.0). The activation energy of 106 kJ mol$^{-1}$ is very close to activation energy of reaction (1b), 108 kJ mol$^{-1}$. At 200°C for example, $k_{8.0 \text{ (phosphite)}} = 1.8\ k_{8.1 \text{ (phosphonite)}}$. The more the temperature increases, the more the difference decreases. Phosphite decomposes faster hydroperoxide than phosphonite but when all phosphite is consumed, there is a small amount of phosphonite which still protects PP against thermal oxidation, according to previous remark (see Table III).

Phosphonite hydrolysis creates BH which acts with $PO_2^{\bullet}$ as a radical chain terminator (reaction 7.1). Activation energy of
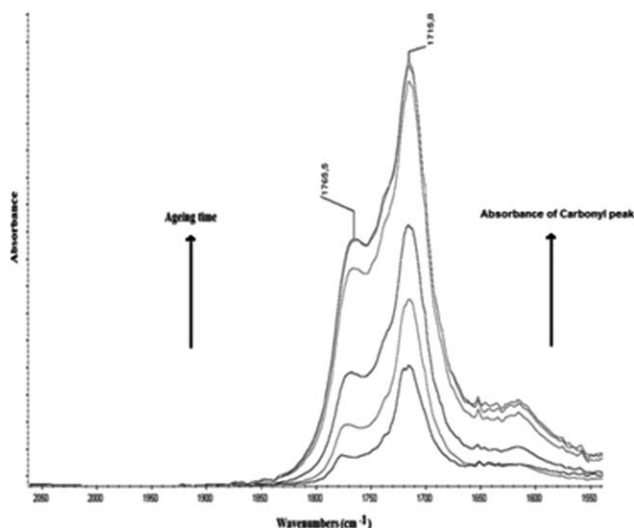
**Figure 3.** IR spectra obtained during the ageing of unstabilized PP at 250°C.

**Table III.** OIT of the PP Samples Studied During the Ageing in Isothermal Condition for Temperature Ranging from 200 to 250°C

| $T$ (°C) | OIT "net PP" (min) | OIT "PP + phosphite" (min) | OIT "PP + phosphonite" (min) |
|---|---|---|---|
| 200 | 11 | >30 | >30 |
| 210 | 5.5 | 20 | >30 |
| 220 | 3 | 6.5 | 18 |
| 230 | 2 | 3 | 8 |
| 240 | 1.5 | 2 | 4.5 |
| 250 | 1 | 2 | 2 |

(7.1) is higher than that of reaction (7.0), that is, 20.5 kJ mol$^{-1}$ and still lower than $E_{a(3)}$ (i.e., 65 kJ mol$^{-1}$). The Hydrogen from BH is less labile than those of phenolic compounds, according to literature[53] but still more unstable than methyne group of PP. From this, dissociation energy of C—H bond from BH can be deduced: 355–380 kJ mol$^{-1}$. From different constant values obtained a in previous study,[67] it is also possible to estimate that $k_{7.0} = 3 - 4\ k_{7.1}$ for 200–250°C at lower temperatures ($T < 100$°C). Literature shows that $k_{7.0} = 10–100\ k_{7.1}$.[53] This ratio decreases with increasing temperature.

Next step will to couple this chemical model with the thermal model, which predicts evolution of polymer temperature during rotational molding, so as to estimate the DCT of different stabilized PP grades during rotational molding.

### In Real Thermal Condition During Rotational Molding
In this section, the two previous stabilized PP grades were tested with following thermal conditions (see Figure 7). The various
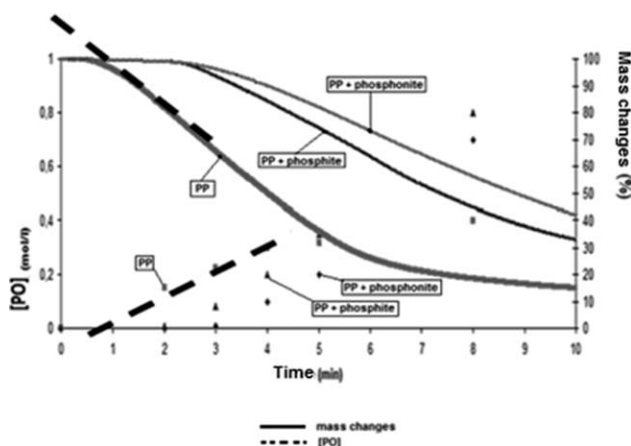
operating conditions differ only by heating time (between 20 and 35 min). All other parameters remain identical [i.e., cooling time in open air (20 min) and rotation speeds around main axis (9.6 rpm) and around secondary axis (4 rpm)]. Then, the thermal model was coupled with the previous chemical model. Figure 8 compares distribution of [P=O] in thickness of stabilized PP rotomolded parts.

Note that for a heating time ($t_c$) of 20 min, PP stabilized with phosphite or phosphonite are not thermally degraded. Maximum [P=O] concentration is under sensitivity threshold of IR equipment ($\approx 10^{-2}$ mol L$^{-1}$). For $t_c = 25$ min, PP stabilized with phosphite or phosphonite are degraded. According to previous remarks, beyond a DCT of 215°C, phosphite seems not effective against PP thermal oxidation and parts are degraded. However, in contrast with previous remarks, phosphonite is not effective against thermal degradation above 215°C (in rotational molding thermal condition). Oxidized layer thickness (TOL) of corresponding rotomolded parts are 70 and 35 μm for "PP + phosphite" and "PP + phosphonite" respectively. For $t_c > 25$ min, these two antioxidants do not protect PP. However, TOL of rotomolded part with "PP + phosphonite" (TOL$_{PP + phosphonite}$) is smaller than that with "PP + phosphite" (TOL$_{PP + phosphite}$). At 30 min for example, TOL$_{PP + phosphonite} = 90$ μm $<$ TOL$_{PP + phosphite} = 110$ μm. The more the temperature increases, the more the difference between TOL decreases until



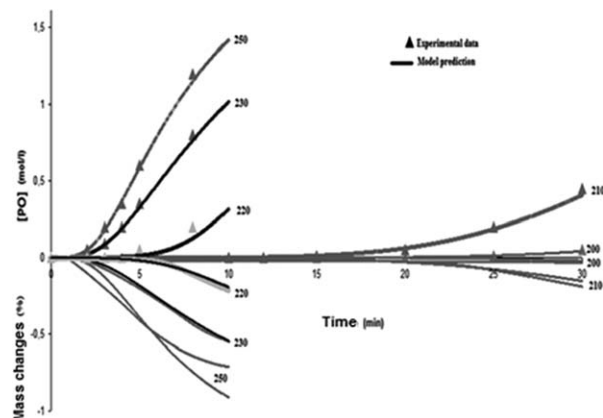**Figure 4.** PO concentration evolutions and mass changes during ageing of the PP samples studied at 250°C.



**Figure 5.** Comparison of experimental and calculated [PO] and mass changes during the ageing in isothermal condition of PP stabilized with phosphite.

**Table IV.** Arrhenius Parameter Values of Elementary Rate Constants for PP Thermal Oxidation Kinetic Between 200 and 250°C

| $k$ | $E_a$ (kJ mol$^{-1}$) | $k_0$ |
|-----|-----|-----|
| 1u | 149 | $5.3 \times 10^{13}$ (s$^{-1}$) |
| 1b | 108 | $10^9$ (L mol$^{-1}$ s$^{-1}$) |
| 2 | 0 | $10^8$ (L mol$^{-1}$ s$^{-1}$) |
| 3 | 65.5 | $3 \times 10^8$ (L mol$^{-1}$ s$^{-1}$) |
| 4 | 0 | $10^{10}$ (L mol$^{-1}$ s$^{-1}$) |
| 5 | 0 | $10^9$ (L mol$^{-1}$ s$^{-1}$) |
| 6.0 | 82 | $7.8 \times 10^{13}$ (L mol$^{-1}$ s$^{-1}$) |
| 6.1 | 20 | $5.9 \times 10^8$ (s$^{-1}$) |
| 6.3 | 25 | $2.3 \times 10^9$ (s$^{-1}$) |
| 8.0 | 80 | $1.2 \times 10^{10}$ (L mol$^{-1}$ s$^{-1}$) |

$E_a$ corresponds to activation energy and $k_0$ at pre-exponential factor.

**Table V.** Arrhenius Parameter Values of Stabilization Reaction Constant by Phosphonite for PP Thermal Oxidation Kinetics Between 200 and 250°C

| $K$ | $E_a$ (kJ mol$^{-1}$) | $k_0$ |
|-----|-----|-----|
| 8.1 | 106 | $5 \times 10^{12}$ (L mol$^{-1}$ s$^{-1}$) |
| 9 | 139 | $2.3 \times 10^{13}$ (L mol$^{-1}$ s$^{-1}$) |
| 7.1 | 33 | $2 \times 10^8$ (L mol$^{-1}$ s$^{-1}$) |

$E_a$ corresponds to activation energy and $k_0$ at pre-exponential factor.

was estimated for PP stabilized with phosphonite/hindered phenol antioxidants. In order to optimize rotational molding, this difference is significant. Also, note in Figure 9 that TOL from "PP + phosphonite + hindered phenol" is smaller than TOL from "PP + phosphonite". At $t_c = 30$ min for example, TOL$_{PP + phosphonite + hindered\ phenol} = 40\ \mu$m < TOL$_{PP + phosphonite} = 90$ μm. The more the temperature increases the more the gap between TOL decreases.
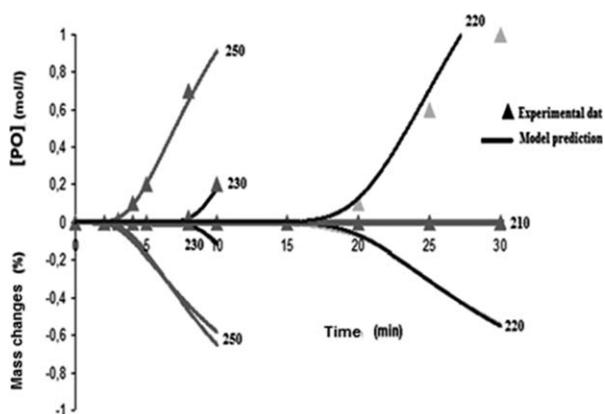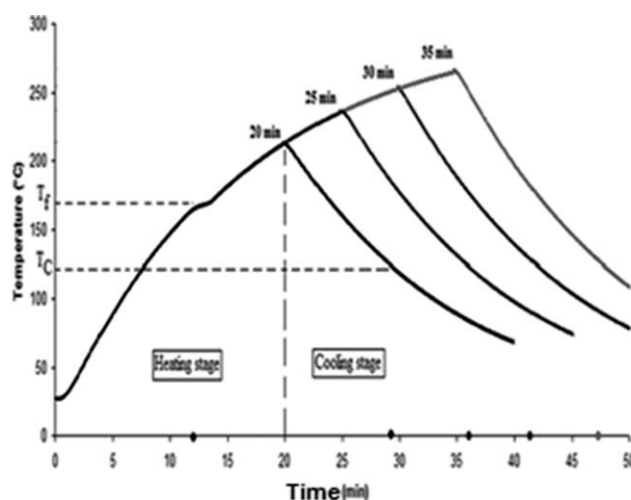
obtaining a similar value for last operating condition ($t_c = 35$ min), TOL$_{PP + phosphonite}$ = TOL$_{PP + phosphite}$.

Finally, the effect of the addition of a radical chain terminator antioxidant against PP thermal degradation during rotational molding was investigated. For this purpose, reaction (7.0) was added to mechanism scheme:

$$PO_2^{\cdot} + AH \rightarrow POOH + A^{\cdot} \qquad (7.0)$$

Initial concentration of hindered phenol, noted [AH]$_0$, is $6.2 \times 10^{-3}$ mol L$^{-1}$. Kinetic constants of reaction (7.0) were deduced from literature.[39,67] Figure 9 compares TOL from PP parts stabilized with phosphonite/hindered phenol or phosphonite/hindered phenol antioxidants for different heating times during processing ($t_c = 25$, 30, or 35 min).

For $t_c = 25$ min, PP stabilized with phosphonite/ hindered phenol is not degraded while PP stabilized with phosphonite is degraded (TOL$_{PP + phosphonite} = 35\ \mu$m). A new DCT of 235°C

## CONCLUSIONS

It was shown in a previous work that the DCT of PP stabilized with a mixture of phosphite and hindered phenol is 215°C (i.e., 20 min heating at an oven temperature of 300°C). In this work, the DCT of the same PP stabilized with phosphonite and same hindered phenol was found to be 235°C (i.e., 25 min heating at an oven temperature of 300°C). To optimize rotational molding, this difference of 5 min is significant. Actually, rotational molding optimization is based on cycle time decreasing (i.e., increasing oven temperature for decreasing heating time). For that, an original coupling between a thermal model able to predict, at any point of rotational molding equipment, the evolution of temperature, and a kinetic model able to predict stabilized



**Figure 6.** Comparison between calculated and experimental evolution of [PO] and mass losses during the isothermal ageing of PP stabilized with phosphonite for temperatures ranging from 200 to 250°C.



**Figure 7.** Calculated $Tt$ diagram obtained during the stabilized PP rotational molding with following operating conditions: oven temperature 300°C, different heating times ($t_c$) = 20, 25, 30, or 35 min and cooling time = 20 min.
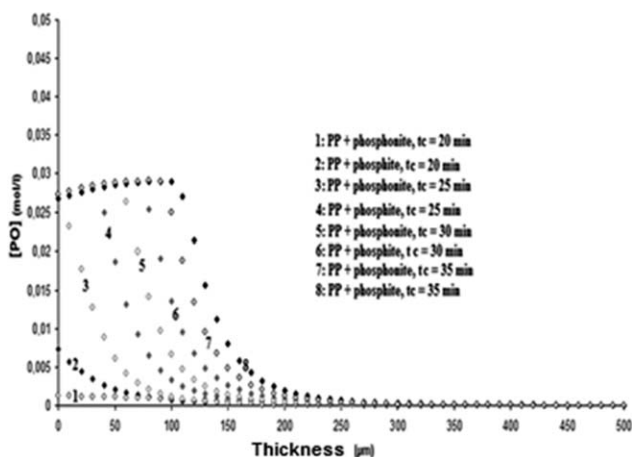
**Figure 8.** Comparison of [PO] distribution through the thickness of roto-molded parts for PP stabilized with phosphite and PP stabilized with phosphonite.

molten state PP thermal oxidation was implemented. From a kinetic viewpoint, phosphite decomposes hydroperoxide faster than phosphonite. However, hydrolysis product of phosphonite (noted BH) acts as a radical chain terminator and blocks the propagation reaction of thermal oxidation. Moreover, activation energy of BH stabilization reaction (7.1) is higher than AH reaction (7.0) and lower than PH consumption reaction (3). Thus, Hydrogen from BH is less labile than Hydrogen from AH but still more unstable than Hydrogen from PH. In other words, dissociation energy of C—H bond from BH can be evaluated between 355 and 380 kJ mol$^{-1}$. Finally, from the different constant values obtained, it was possible to estimate the $k_{7.0}$ / $k_{7.1}$ ratio, which increases with decreasing temperature ($k_{7.0}/k_{7.1} = $ 3–4 for $T = 200$–$250°C$, whereas at $T < 100°C$, $k_{7.0}/k_{7.1} = 10$–$100$).
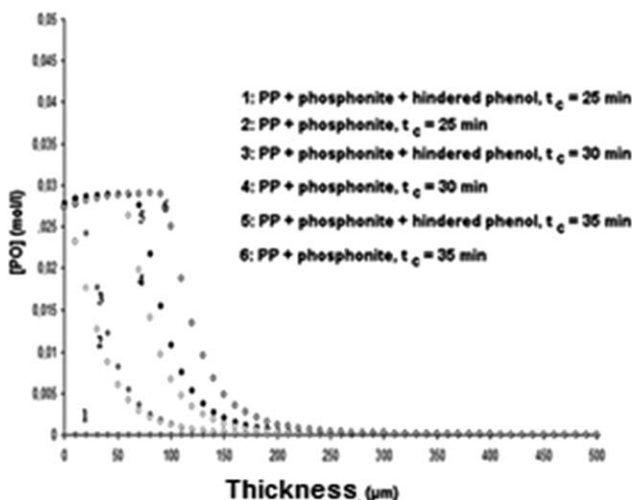


**Figure 9.** Comparison of [PO] distribution in thickness of rotomolded parts for PP stabilized with phosphonite and for PP stabilized with phosphite and hindered phenol.

## APPENDIX: FROM STANDARD SCHEME EXTENDED TO MOLTEN POLYPROPYLENE STABILIZED BY PHOSPHONITE AND HINDERED PHENOL

$$\frac{d[P^{\bullet}]}{dt} = 2k_{1u}f_{PH}[POOH] + k_{1b}f_{PH}[POOH]^2 - k_2[P^{\bullet}][O_2] + k_3[PO_2^{\bullet}][PH] - 2k_4[P^{\bullet}]^2 - k_5[P^{\bullet}][PO_2^{\bullet}] + 2k_{6.3}f_{PH}[PO^{\bullet\bullet}OP^{\bullet}]$$
(A1)

$$\frac{d[PO_2^{\bullet}]}{dt} = k_{1b}\ f_{PH}[POOH]^2 + k_2[P^{\bullet}][O_2] - k_3[PO_2^{\bullet}][PH] - k_5[P^{\bullet}][PO_2^{\bullet}] - 2k_{6.0}[PO_2^{\bullet}]^2 - n_{AH}k_{7.0}[PO_2^{\bullet}][AH] - n_{BH}k_{7.1}[PO_2^{\bullet}][BH]$$
(A2)

$$\frac{d[POOH]}{dt} = -k_{1u}f_{PH}[POOH] - 2k_{1b}f_{PH}[POOH]^2 + k_3[PO_2^{\bullet}][PH] + (1-\gamma_5)\ k_5\ [P^{\bullet}][PO_2^{\bullet}] - k_{8.1}[POOH][Dec] + n_{AH}k_{7.0}[PO_2^{\bullet}][AH] + n_{BH}k_{7.1}[PO_2^{\bullet}][BH]$$
(A3)

$$\frac{d[PO^{\bullet\bullet}OP]}{dt} = k_{6.0}[PO_2^{\bullet}]^2 - (k_{6.1} + k_{6.3}f_{PH})[PO^{\bullet\bullet}OP]$$
(A4)

$$\frac{d[PH]}{dt} = -(2-\gamma1 + n_{PH}.v)k_{1u}f_{PH}[POOH] - (1-\gamma1 + n_{PH}.v)k_{1b}f_{PH}[POOH]^2 - k_3[PO_2^{\bullet}][PH] + (1-\gamma_4)k_4[P^{\bullet}]^2 - 2.(1+n_{PH}.v)k_{6.3}f_{PH}[PO^{\bullet\bullet}OP]$$
(A5)

$$\frac{\partial[O_2]}{\partial t} = D_{O2}\frac{\partial^2[O_2]}{\partial x^2} - k_2[P^{\bullet}][O_2] + k_{6.0}[PO_2^{\bullet}]^2$$
(A6)

$$\frac{\partial[Dec]}{\partial t} = D_{Dec}\frac{\partial^2[Dec]}{\partial x^2} - k_{8.1}[POOH][Dec] - k_9[H_2O][Dec]$$
(A7)

$$\frac{\partial[AH]}{\partial t} = D_{AH}\frac{\partial^2[AH]}{\partial x^2} - n_{AH}k_{7.0}[PO_2^{\bullet}][AH]$$
(A8)

$$\frac{\partial[BH]}{\partial t} = D_{BH}\frac{\partial^2[BH]}{\partial x^2} + n_{BH}k_9[H_2O][Dec] - n_{BH}k_{7.1}[PO_2^{\bullet}][BH]$$
(A9)

$$\frac{\partial[H_2O]}{\partial t} = k_{1H}f_{PH}[POOH] + k_{1b}f_{PH}[POOH]^2 - k_9[Dec][H_2O]$$
(A10)

$$\frac{\partial[PP]}{\partial t} = \gamma_4 k_4[P^{\bullet}]^2$$
(A11)

$$\frac{\partial[F]}{\partial t} = (1-\gamma_4)k_4[P^{\bullet}]^2 + (1-\gamma_5)k_5[P^{\bullet}][PO_2^{\bullet}]$$
(A12)

$$\frac{\partial[\text{POOP}]}{\partial t} = \gamma_5 k_5 [\text{P}^\bullet][\text{PO}_2^\bullet] + k_{6.1}[\text{PO}^{\bullet\bullet}\text{OP}] \qquad (A13)$$

$$\frac{d[\text{P}=\text{O}]}{dt} = (\gamma_1 - n_{\text{CO}}.v)k_{1u}f_{\text{PH}}[\text{POOH}] + (\gamma_1 - n_{\text{CO}}.v)k_{1b}f_{\text{PH}}[\text{POOH}]^2$$
$$+ 2.(\gamma_1 - n_{CO}.v)k_{6.3}f_{\text{PH}}[\text{PO}^{\bullet\bullet}\text{OP}] \qquad (A14)$$

$$\frac{d[\text{P}-\text{OH}]}{dt} = -(\gamma_1 + n_{\text{OH}}.v)k_{1u}f_{\text{PH}}[\text{POOH}]$$
$$- (1 + \gamma_1 + n_{\text{OH}}.v)k_{1b}f_{\text{PH}}[\text{POOH}]^2 + k_3[\text{PH}][\text{PO}_2^\bullet]$$
$$+ (1 - \gamma_5)k_5[\text{P}^\bullet][\text{PO}_2^\bullet] + 2(1 - \gamma_1 - n_{\text{OH}}.v)k_{6.3}f_{\text{PH}}[\text{PO}^{\bullet\bullet}\text{OP}]$$
$$- k_{8.1}[\text{POOH}][\text{Dec}] + k_{7.1}[\text{PO}_2^\bullet][\text{BH}] + k_{7.0}[\text{PO}_2^\bullet][\text{AH}] \qquad (A15)$$

$$\frac{1}{m_0}\frac{dm}{dt} = + \frac{32}{\rho_T}\frac{d[\text{O}_2]}{dt} - \frac{18}{\rho_T}\frac{d[\text{H}_2\text{O}]}{dt} - \frac{M_V}{\rho_T}\frac{d[V]}{dt}$$
$$\frac{1}{m_0}\frac{dm}{dt} = \frac{32}{\rho_T}(-k_2[\text{O}_2][\text{P}^\bullet] + k_{6.0}[\text{PO}_2^\bullet]^2)$$
$$- \frac{18}{\rho_T}(k_{1u}f_{\text{PH}}[\text{POOH}] + k_{1b}f_{\text{PH}}[\text{POOH}]^2 - k_9[\text{Dec}][\text{H}_2\text{O}])$$
$$- v.\frac{M_V}{\rho_T}(k_{1u}f_{\text{PH}}[\text{POOH}] + k_{1b}f_{\text{PH}}[\text{POOH}]^2$$
$$+ 2.k_{6.3}f_{\text{PH}}[\text{PO}^{\bullet\bullet}\text{OP}]) \qquad (A16)$$

- $f_{\text{PH}}$ a mathematical function introduced to avoid that concentration of substrate becomes negative, $f_{\text{PH}} = \dfrac{[\text{PH}]}{[\text{PH}] + \varepsilon}$ with $\varepsilon = 10^{-2}$,[18]
- $D_{\text{O2}}$ diffusion coefficient of oxygen $D_{\text{O2}} = 4.6 \times 10^{-3}\exp\left(-\frac{47700}{RT}\right)$,[18]
- $D_{\text{Dec}}$ diffusion coefficient of preventive antioxidants $D_{\text{Dec}} = 1.9 \times 10^3 \exp\left(-\frac{94000}{RT}\right)$,[67]
- $D_{\text{AH}}$ diffusion coefficient of phenol antioxidant $D_{\text{AH}} = 4.6 \exp\left(-\frac{100000}{RT}\right)$,[67]
- $D_{\text{BH}}$ diffusion coefficient of phenol antioxidant $D_{\text{BH}} = 4.6 \exp\left(-\frac{100000}{RT}\right)$,
- $\rho_T$ is molten polymer density at temperature $T$. For example, $\rho_{473K} = 832$ g L$^{-1}$.[18]
- $[\text{P}^\bullet]_0 = [\text{PO}_2^\bullet]_0 = [\text{PO}^{\bullet\bullet}\text{OP}]_0 = [\text{BH}]_0 = [\text{H}_2\text{O}]_0 = [\text{PP}]_0 = [\text{F}]_0 = [\text{POOP}]_0 = [\text{P}=\text{O}]_0 = [\text{POH}]_0 = [V]_0 = 0$ mol L$^{-1}$.
- $[\text{POOH}]_0 = 0.001$ mol L$^{-1}$; $[\text{PH}]_0 = 20.3$ mol L$^{-1}$; $[\text{AH}]_0 = 0.0062$ mol L$^{-1}$;
- $[\text{Dec}]_0 = 0.01$ mol L$^{-1}$ $[\text{O}_2]_0 = 0.001$ mol L$^{-1}$.
- $\gamma_1 = 90 - 99.9\%$; $\gamma_4 = 16\%$; $\gamma_5 = 50\%$; $v = 84.7 - 88\%$.
- $M_v = 58$ g mol$^{-1}$; $n_{\text{CO}} = 1$; $n_{\text{OH}} = n_{\text{PH}} = 0$; $n_{\text{AH}} = n_{\text{BH}} = 4$; $\beta_{\text{Dec}} = \beta_{\text{AH}} = \beta_{\text{BH}} = 0.00001$ s$^{-1}$; $R = 8.31$ J mol$^{-1}$ K$^{-1}$.

## REFERENCES

1. Zweifel, H.; Maier, R.; Schiller, M. Plastics Additives Handbook, 6th ed.; Hanser Publishers: Munich, **2009**.

2. Bolland, J. L.; Gee, G. *Trans. Faraday Soc.* **1946**, *42*, 244.

3. Audouin, L.; Achimsky, L.; Verdu J. Handbook of Polymer Degradation, 2nd ed.; Marcel Dekker: New York, **2000**.

4. Bolland, J. L.; Gee, G. *Trans. Faraday Soc.* **1946**, *42*, 236.

5. Rincon Rubio, L.; Fayolle, B.; Audouin, L.; Verdu, J. *Polym. Degrad. Stab.* **2001**, *74*, 177.

6. Reich, L.; Stivala, S. S. Oxidation of Simple Hydrocarbons in the Absence of Inhibitors and Accelerators. Autooxidation of Hydrocarbons and Polyolefins, Kinetics and Mechanisms; Marcel Dekker: New York, **1969**.

7. Colin, X.; Fayolle, B.; Audouin, L.; Verdu, J.; Duteurtre, S. Vieillissement thermo-oxydant des polymères. Un pas vers la modélisation cinétique. Vieillissement et durabilité des matériaux; Lavoisier Tec&Doc: Paris, **2003**.

8. Richaud, E.; Farcas, F.; Bartolomeo, P.; Fayolle, B.; Audouin, L.; Verdu, J. *Polym. Degrad. Stab.* **2005**, *91*, 398.

9. El-Mazry, C.; Ben Hassine, M.; Correc, O.; Colin, X. *Polym. Degrad. Stab.* **2013**, *98*, 22.

10. Verdu, S.; Verdu, J. *Macromolecules* **1997**, *30*, 2262.

11. Colin, X.; Fayolle, B.; Audouin, L.; Verdu, J. *Polym. Degrad. Stab.* **2003**, *80*, 67.

12. Colin, X.; Audouin, L.; Verdu, J. *Polym. Degrad. Stab.* **2007**, *92*, 886.

13. Coquillat, M.; Verdu, J.; Colin, X.; Audouin, L.; Nevière, R. *Polym. Degrad. Stab.* **2007**, *92*, 1326.

14. Boss, C. R.; Chien, J. C. W. *J. Polym. Sci. Part A-1: Polym. Chem.* **1966**, *4*, 1543.

15. Billingham, N. C.; Calvert, P. D. Developments in Polymer Stabilization; Applied Science. Scott: London, **1980**.

16. Gillen, K. T.; Wise, J.; Clough, R. L. *Polym. Degrad. Stab.* **1995**, *47*, 149.

17. Fayolle, B.; Audouin, L.; George, G. A.; Verdu, J. *Polym. Degrad. Stab.* **2002**, *77*, 515.

18. Sarrabi, S.; Colin, X.; Tcharkhtchi, A. *J. Appl. Polym. Sci.* **2008**, *110*, 2030.

19. Sarrabi, S.; Colin, X.; Tcharkhtchi, A.; Heninger, M.; Leprovost, J.; Mestdagh, H. *Anal. Chem.* **2009**, *81*, 6013.

20. Howard, J. A.; Ingold, K. U. *Can. J. Chem.* **1968**, *46*, 2655.

21. Russel, G. A. *J. Am. Chem. Soc.* **1956**, *78*, 1047.

22. Achimsky, L. Etude cinétique de la thermooxydation du polypropylène. Ph.D. Thesis, ENSAM, Paris, **1996**.

23. Frank, H. P. *J. Polym. Sci.: Polym. Symp.* **1976**, *57*, 311.

24. Allen, N. S.; Hoang, E.; Liauw, C. M.; Edge, M.; Fontan, E. *Polym. Degrad. Stab.* **2001**, *72*, 367.

25. Gensier, R.; Plummer, C. J. G.; Kausch, H. H.; Kramer, E.; Pauquet, J. R.; Zweifel, H. *Polym. Degrad. Stab.* **2000**, *67*, 195.

26. Tochacek, J. *Polym. Degrad. Stab.* **2004**, *86*, 385.

27. Richaud, E.; Fayolle, B.; Verdu, J. *Polym. Degrad. Stab.* **2011**, *96*, 1.

28. Ramani, R.; Alam, S. *Thermochim. Acta* **2012**, *550*, 33.

29. Pospisil, J.; Horak, Z.; Pilar, J.; Billingham, N. C.; Zweifel, H.; Nespurek, S. *Polym. Degrad. Stab.* **2003**, *82*, 145.

30. Ismail, M. N.; Yehia, A. A.; Korium, A. A. *Polym. Degrad. Stab.* **2001**, *74*, 274.

31. Kamiya, Y.; Niki, E.; Jellinek, H. H. G. Oxidative Degradation; Elsevier Scientific Publishing Company: Amsterdam, **1978**.

32. Shelton, R. J.; Hawkins, W. L. Polymer Stabilization; Wiley Interscience: New York, **1971**.

33. Zweifel, H. Plastics Additives Handbook, 5th ed.; Hanser Publishers: Munich, **2001**.

34. Bordwell, F. G.; Zhang, X. M. *J. Phys. Org. Chem.* **1995**, *8*, 529.

35. Mulder, P.; Saastad, O. W.; Griller, D. *J. Am. Chem. Soc.* **1988**, *110*, 4090.

36. Zhu, Q.; Zhang, X. M.; Fry, A. *J. Polym. Degrad. Stab.* **1997**, *57*, 43.

37. Pospíšil, J. *Polym. Degrad. Stab.* **1993**, *40*, 217.

38. Pospíšil, J. *Polym. Degrad. Stab.* **1993**, *39*, 103.

39. Gol'dberg, V. M.; Vidovskaya, L. M.; Zaikov, G. E. *Polym. Degrad. Stab.* **1988**, *20*, 93.

40. Hsuan, C. Y. G.; Koerner, R. M. *J. Geotech. Geoenviron. Eng.* **1988**, *124*, 532.

41. Kriston, I.; Orbán-Mester, A.; Nagy, G.; Staniek, P.; Földes, E.; Pukánszky, B. *Polym. Degrad. Stab.* **2009**, *94*, 1448.

42. Kriston, I.; Pénzes, G.; Szijjártó, G.; Szabó, P.; Staniek, P.; Földes, E.; Pukánszky, B. *Polym. Degrad. Stab.* **2010**, *95*, 1883.

43. Kriston, I.; Orbán-Mester, A.; Nagy, G.; Staniek, P.; Földes, E.; Pukánszky, B. *Polym. Degrad. Stab.* **2009**, *94*, 719.

44. Pénzes, G.; Domjan, A.; Tatraaljai, D.; Staniek, P.; Földes, E.; Pukánszky, B. *Polym. Degrad. Stab.* **2010**, *95*, 1627.

45. Tochacek, J.; Jancar, J. *Polym. Test.* **2012**, *31*, 1115.

46. Hiatt, R.; Smythe, R. J.; McColeman, C. *Can. J. Chem.* **1971**, *49*, 1707.

47. Scott, G. *Pure Appl. Chem.* **1972**, *30*, 267.

48. Schwetlick, K.; Pionteck, J.; König, T.; Habicher, W. D. *Eur. Polym. J.* **1987**, *23*, 383.

49. Habicher, W. D.; Bauer, I.; Halim, H. Handbook of Polymer Degradation, 2nd ed.; Marcel Dekker Inc.: New York, **2000**.

50. Schwetlick, K.; Habicher, W. D.; Clough, R. L.; Billingham, N. C.; Gillen, K. T. Polymer durability: Degradation, stabilization, and lifetime prediction; American Chemical Society: Washington, **1996**.

51. Al Malaika, S.; Peng, X. *Polym. Degrad. Stab.* **2008**, *93*, 1619.

52. Costanzi, D.; Farris, R.; Girelli, D. *Polym. Degrad. Stab.* **2001**, *73*, 425.

53. Schwetlick, K.; König, T.; Pionteck, D.; Sasse, D.; Habicher, W. D. *Polym. Degrad. Stab.* **1988**, *22*, 357.

54. Parrondo, A.; Allen, N. S.; Edge, M.; Fontan, E. *Polym. Degrad. Stab.* **2001**, *72*, 367.

55. Habicher, W. D.; Bauer, I.; Pospíšil, J. *Macromol. Symp.* **2005**, *225*, 147.

56. Crawford, R. J. Rotational Moulding of Plastic, 2nd ed.; Research Studies Press Ltd: New York, **1996**.

57. Tcharkhtchi, A. Rotomoulage de pièces en matière thermoplastique; Techniques de l'ingénieur: Paris, **2004**.

58. Crawford, R. J.; Nugent, P. J. *Plast. Rubber Compos. Process. Appl.* **1992**, *17*, 33.

59. Crawford, R. J.; Nugent, P. J. *Plast. Rubber Compos. Process. Appl.* **1992**, *17*, 23.

60. Throne, J. L. *Polym. Eng. Sci.* **1972**, *12*, 335.

61. Sun, D. W.; Crawford, R. J. *Plast. Rubber Compos. Process. Appl.* **1993**, *19*, 47.

62. Nugent, P. A study of heat transfer and process control in the rotational moulding of polymer powders, Ph.D. Thesis, The Queen's University, Belfast, **1990**.

63. Olson, L. G.; Crawford, R. J.; Kearns, M.; Geiger, N. *Polym. Eng. Sci.* **2000**, *40*, 1758.

64. Gogos, G.; Olson, L. G.; Liu, X.; Pasham, V. R. *Polym. Eng. Sci.* **1998**, *38*, 1387.

65. Tcharkhtchi, A.; Pérot, E.; Chinesta, F. *Int. Polym. Process.* **2004**, *3*, 296.

66. Sarrabi, S.; Boyer, S. A. E.; Lacrampe, M. F.; Krawczak, P.; Tcharkhtchi, A. *J. Appl. Polym. Sci.* **2013**, *130*, 222.

67. Sarrabi, S.; Colin, X.; Tcharkhtchi, A. *J. Appl. Polym. Sci.* **2010**, *118*, 980.

68. Verdu, J. Vieillissement des plastiques; AFNOR: Paris, **1984**.

69. Samuels, R. J. Structured Polymers Properties; Wiley: New York, **1974**.

70. Teissèdre, G.; Pilichowski, J. F.; Lacoste, J. *Polym. Degrad. Stab.* **1994**, *45*, 145.

71. George, G. A.; Celina, M.; Vassallo, A. M.; Cole-Clarke, P. A. *Polym. Degrad. Stab.* **1995**, *48*, 199.

72. Adams, J. H. *J. Polym. Sci. Part A-1: Polym. Chem.* **1970**, *8*, 1077.

73. Lacoste, J.; Vaillant, D.; Carlsson, D. J. *J. Polym. Sci. Part A-1: Polym. Chem.* **1993**, *31*, 715.

74. Ohwada, K. *Appl. Spectrosc.* **1968**, *22*, 209.

75. Földes, E.; Maloschik, E.; Kriston, I.; Staniek, P.; Pukánszky, B. *Polym. Degrad. Stab.* **2006**, *91*, 479.

76. Djouani, F.; Richaud, E.; Fayolle, B.; Verdu, J. *Polym. Degrad. Stab.* **2011**, *96*, 1349.

77. Philippart, J. L.; Sinturel, C.; Arnaud, R.; Gardette J. L. *Polym. Degrad. Stab.* **1999**, *64*, 213.

78. Richaud, E.; Farcas, F.; Fayolle, B.; Audouin, L.; Verdu, J. *Polym. Degrad. Stab.* **2006**, *92*, 118.

79. Korcek, S.; Chenier, J. H. B.; Howard, J. A.; Ingold, K. U. *Can. J. Chem.* **1972**, *50*, 2285.

80. Colin, X.; Audouin, L.; Verdu, J. *Polym. Degrad. Stab.* **2004**, *86*, 309.

81. Colin, X.; Audouin, L.; Verdu, J.; Le Huy, M. *Polym. Degrad. Stab.* **2007**, *92*, 898.

82. Colin, X.; Audouin, L.; Verdu, J. *Polym. Degrad. Stab.* **2007**, *92*, 906.

83. Khelidj, N.; Colin, X.; Audouin, L.; Verdu, J.; Monchy-Leroy, C.; Prunier, V. *Polym. Degrad. Stab.* **2006**, *91*, 1598.